Bioorganic Chemistry 104 (2020) 104248

Contents lists available at ScienceDirect

Bioorganic Chemistry

journal homepage: www.elsevier.com/locate/bioorg

Anticandidal formyl phloroglucinol meroterpenoids: Biomimetic synthesis and *in vitro* evaluation

Lin–Fang Zhong, Zhi–Chun Shang, Fu–Juan Sun, Pan–Hu Zhu, Yong Yin, Ling–Yi Kong*, Ming–Hua Yang*

Jiangsu Key Laboratory of Bioactive Natural Product Research and State Key Laboratory of Natural Medicines, School of Traditional Chinese Pharmacy, China Pharmaceutical University, Nanjing 210009, People's Republic of China

ARTICLE INFO

Keywords:
Formyl phloroglucinol meroterpenoids
Essential oil
Anticandidal activity
Antibiofilm activity

ABSTRACT

Inspired by the diversity-oriented synthesis, some novel formyl phloroglucinol meroterpenoids were synthesized via biomimetic synthesis using essential oils. Eight of them were demonstrated with good *in vitro* fungicidal activity against *Candida albicans* and *C. glabrata*. Compound **c2** showed the best anticandidal ability that was powerfully comparable to fluconazole when testing against several strains *in vitro*. The antibiofilm activity was also found for the **c2** treating group which was evidenced to block the hyphal elongation and filamentation of *C. albicans*. Therefore, compound **c2** is a promising candidate for further antifungal-based structure modification.

1. Introduction

Natural products have long been considered a potential source of novel drug leads on all sides. The development of antifungals benefits a lot from nature too [1–2]. The echinocandin is the product of *Aspergillus nidulans* and the amphotericin B and nystatin (polyenes) are naturally occurring polyethylenes in different *Streptomyces* species [3–6]. However, there are relatively a few classes of antifungals used in clinic and most of them have been using for decades [7–8]. Their widespread and prolonged application leads to the increasingly severe drug resistance problem in clinic [9–10]. Developing drugs with novel antifungal targets is one of most useful solutions. Natural products with various and novel structure are still wonderful candidate pool, and some molecules with novel targets like caspofungin and celastrol already shown their perfect application prospects in recent researches [11].

Formyl phloroglucinol meroterpenoids (FPMs) are characteristic metabolites of the genus *Eucalyptus*. They are the phloroglucinol hybrids of terpene moieties and structurally diverse in the terpenoid types plus conjugate patterns [12–14]. Our previous research on the leaves of *Eucalyptus robusta* Smith was resulted in a lot of FPMs with potential anticandidal activity against different *Candida* spp., including fluconazole-resistant strains [15–17]. Some of them exerted a strong inhibitory effect against *C. albicans* biofilms, and some showed synergistic effect with azoles [18–19]. These qualities make FPMs potential candidates for antifungal agents. Analyzing the anticandidal structure-activity relationships, we found that only three terpene types could provide obvious anticandidal activity to FPMs, although more than ten types with different hybrid patterns were found. The terpenoid involved in forming FPMs undoubtedly is one of the key elements concerning their antifungal ability. If we were able to screen FPMs with more different terpenes, it was possible to find more effective candidates.

Terpenoids were found to be potential efflux pump substrates of fungi, which was evidenced by the fact that they were active against efflux pump-deficient *C. albicans* but inert towards wild-type strains [20]. It means they cannot be intracellularly retained enough to inhibit or kill general fungal strains. Structural modification employing organelle-targeting groups was proved to be a useful way to enhance or restore the drug activity [21–22]. Several terpenoids were restored their anticandidal activity by conjugating them to the mitochondria-targeting triphenylphosphonium cation [20]. The endoplasmic reticulum-localized azole was also reported to remarkably improve antifungal activity against a panel of *Candida* spp. [23]. In light of above findings, we posited that the phloroglucinol group in FPMs could have exerted a retaining effect to terpene group too.

More FPMs were desired to discover effective FPMs and to verify our function hypothesis on phloroglucinol group. Different routes had been reported for biomimetic synthesis of FPMs [14,24], which therefore could be an efficient option for us. However, it would be difficult to gather many terpenoids as reagents, and the bioassay screening of abundant products also could be a heavy task. Inspired by the diversity-oriented synthesis [25–27], essential oils with rich terpenes constituents could be ideal reaction reagents. It is because of that different

* Corresponding author.
E-mail addresses: cpu_lykong@126.com (L. Kong), skeepjack@163.com (M. Yang).

https://doi.org/10.1016/j.bioorg.2020.104248
Received 1 March 2020; Received in revised form 15 May 2020; Accepted 28 August 2020
Available online 01 September 2020
0045-2068/

terpenes in them would generate diverse FPMs in one reaction, which combined with bioactivity-guided isolation would improve our efficiency of finding more antifungal FPMs. Hence, we conducted this synthetic strategy by using commercially available essential oil and successfully obtained several novel anticandidal FPMs.

2. Results and discussion

2.1. Chemistry

2.1.1. Biomimetic synthesis of FPMs

The phloroglucinol-terpene adducts are biosynthetically hypothesized to arise from the Diels-Alder (DA) cycloaddition [14,24]. Our previous study had proved that biomimetic synthesis conducting DA conditions was an effective way to produce them [28–30]. Meanwhile, the previous antifungal structure-activity relationships indicated that rather than the single C—C bonds between two moieties, the formation of oxygen heterocycle which is the typical product of DA reaction could contribute to antifungal activity [15–17]. The hetero DA reaction is therefore an appropriate way in this case.

Since the number of terpenes in essential oil is directly related to the variety of FPMs it would produce, we selected 12 essential oils that are different in terpenes as reaction reagents. They were listed in Table S1 along with their plant source. As shown in Table S2, several conditions were investigated to promote the DA reaction. The reaction with the use of sodium acetate (10 equiv) in acetic acid at 100 °C for 16 h obtained a better yield of FPMs' mixture which also showed numbers of peaks in HPLC analysis. This condition was accordingly applied, and the synthetic route was illustrated in Scheme 1.

The 12 essential oils respectively produced 12 crude mixtures of FPMs by conducting the route, and every product was further divided into 4 fractions by silica gel column chromatography. The 48 fractions were then preliminarily submitted to the disk diffusion assay and the anticandidal fractions were double checked by broth microdilution assay. As shown in Table 1, fractions of products derived from cedar oil and ginger oil had the best antifungal activity against the two main pathogens of candidiasis. Their abilities were confirmed by disk diffusion assay (Fig. 1), in which both fractions showed obvious concentration-dependent inhibition zones. Thus, these two fractions were further purified by chromatography which led to the isolation of anticandidal **c1**-**c5** and **g1**-**g3** (Fig. 2) along with the inactive compounds **c6** and **g4**-**g7** (Structures in Fig. S1, and NMR data in Tables S3 and S4). **c1**-**c6** were the product of cedar oil and **g1**-**g7** were isolated from the product of ginger oil. All the isolates were the [4 + 2] cycloaddition products of the conjugated diene from formyl-phloroglucinol and the dienophile from terpenes. The formation of the **c1**-**c5** and **g1**-**g3** were described in scheme 2.

2.1.2. Structure determination of bioactive FPMs

Compound **c1** was determined to have the molecular formula $C_{19}H_{22}O_5$ by HRESIMS. Its ^{1}H NMR data clearly showed the characteristic signals of formyl-phloroglucinol which were the two hydrogen-bonded phenolic hydroxyl groups (δ_H 13.44 and 13.25, each 1H, s) and the two formyl groups (δ_H 10.05 and 10.16, each 1H, s). Aside from those of above moiety and a carbon came from the formaldehyde in reaction, there were 10 carbons left in the ^{13}C NMR spectrum, which revealed a monoterpene moiety for **c1**. The HMBC correlations (Fig. S2) from Me-9 to C-3/C-8, from Me-10 to C-1/C-5/C-6, from H-3 to C-2/C-5, and from H_2-4 to C-2/C-6 revealed a menthane-type monoterpene with the $\Delta^{1(6)}$ double bond. The downfield-shifted C-7 (δ_C 82.7) and the HMBC correlation from H_2-7′ to C-7/C-8/C-3′/C-1′ confirmed that the two moieties were fused through a dihydropyran ring. Obviously, compound **c1** is the adduct of formyl-phloroglucinol and limonene, and a DA addition was happened on the $\Delta^{7(8)}$ double bond of limonene. Compound **c2** was determined as a C-7 epimer of **c1**. It had a same molecular formula and very similar 1D and 2D NMR data to **c1**, but the Me-9 had a ROESY correlation with H-4. This was due to the achiral condition using for the synthesis above.

Compounds **c3** and **c4** were a pair of epimer, since they had the same molecular formula and almost identical NMR data. The HMBC correlations clearly (Fig. S2) revealed that they were also the adducts of limonene, but the $\Delta^{1(6)}$ double bond was involved in fusing with the formyl-phloroglucinol in **c3** and **c4**. The ROESY correlations between H-1/Me-10, H-5α/Me-10, H-3/H-2β, H-3/H-5β and H-1/H-2α were found in **c3**, while **c4** had ROESY correlations between Me-10/H-1 and H-3/H-1. Thus, **c3** and **c4** were C-9 epimers.

The molecular formula $C_{19}H_{22}O_5$ of both **c5** and **g1** revealed that these two synthetic FPMs were a pair of isomers, and the characteristic upfield-shifted H-3 indicated that they were the formyl-phloroglucinol hybrids with the sabinene [31] and its isomers. This was confirmed by the HMBC correlations which also determined the different linkage of two moiety in them (Fig. S2). The HMBC correlations from H_2-7′ to C-6, H_2-10 to C-1, H_2-4 to C-6, H_2-5 to C-3, H_2-2 to C-7, Me-8 to C-3/C-9 and Me-9 to C-3 along with the chemical shift of C-6 (δ_C 91.2) determined the oxa-spiro [5.5] ring in **c5** as the coupling pattern of euglobal Ic [32]. The HMBC correlations from H_2-7′ to C-4/C-5/C-6 revealed that C-5 and C-6 in **g1** were participated in forming the dihydropyran ring with formyl-phloroglucinol. In addition, their relative configurations were determined by the ROESY correlations shown in Fig. S2.

Compounds **g2** and **g3** were determined as the adducts with pinene-type monoterpene, since their NMR data were similar to those of robustadial A [33–34]. The HMBC correlations (Fig. S2) further determined that the double bond of an α-pinene formed the dihydropyran with phloroglucinol in **g2**, and the double bond of a β-pinene formed the oxa-spiro [5.5] ring in **g3**.

The Snatzke helicity rules [15] were used to determine the absolute

Table 1
In vitro anticandidal activity of the best fractions of products derived from 12 essential oils respectively.

Fractions	*C. albicans*[a]	*C. glabrata*[a]
Cedar oil's product	54.90 ± 4.21	80.50 ± 3.26
Spikenard oil's product	129.50 ± 1.23	138.40 ± 2.71
Zedoary oil's product	> 500	196.50 ± 1.21
Citronella's product	> 500	210.20 ± 2.10
Atractylis oil's product	141.60 ± 5.81	137.50 ± 1.24
Ginger oil's product	60.30 ± 3.14	74.80 ± 1.52
Chamomile oil's product	> 500	230.60 ± 2.14
Orange flower oil's product	211.40 ± 1.51	> 500 ± 1.52
Rosemary oil's product	123.50 ± 2.71	190.80 ± 1.71
Lavender oil's product	194.10 ± 0.93	182.10 ± 2.12
Clove oil's product	162.70 ± 4.72	149.30 ± 3.10
Peppermint oil's product	130.10 ± 1.30	125.40 ± 1.31
Fluconazole[b]	0.50 ± 0.13	1.00 ± 0.23

C. albicans (SC5314); *C. glabrata* (ATCC 15126).
[a] MIC_{50} value; μg/mL.
[b] Positive drug.

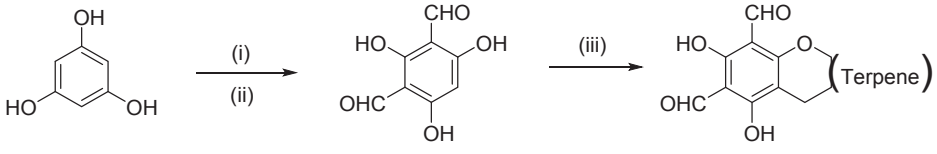

Scheme 1. The synthetic route for FPMs. Reagents and conditions. (i) DMF, $POCl_3$, Dioxane, 12 h, rt; (ii) H_2O, 4 h, 0 °C; (iii) Essential oil, CH_3COOH, CH_3COONa, HCHO, 16 h, 100 °C.

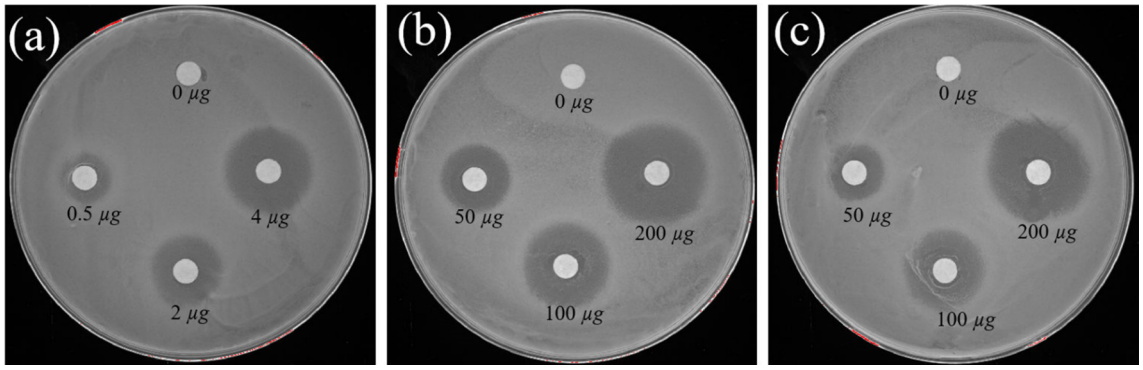

Fig. 1. The anti-*candida albicans* (SC5314) effect of crude fractions in disk diffusion testing. (a) The inhibition zones of fluconazole; (b) The inhibition zones of the best active fraction of cedar oil's product; (c) The inhibition zones of the best active fraction of ginger oil's product.

configuration of above eight compounds. As shown in Fig. S3, each helical direction of dihydropyran rings was predicted according to the signs of the Cotton effects around 280 nm, and therefore those chiral centers on the dihydropyran rings were determined as shown.

2.2. Biological evaluation

2.2.1. In vitro anticandidal activity

All the 13 compounds were evaluated for their *in vitro* anticandidal activity on *C. albicans* and *C. glabrata*. As shown in Table 2, eight compounds showed certain activity. They are all the phloroglucinol adducts of monoterpenes, and these monoterpene precursors were happened to be reported for their antifungal activities before [35]. For example, limonene was reported to inhibit *Candida albicans* growth by inducing apoptosis [36]. However, it is noticed that the limonene adducts, compounds **c1**-**c4**, were much more effective, which could be the contribution from formyl-phloroglucinol. Compounds **c1**-**c4** had a relatively notable influence and thus were submitted to further evaluation. Another four *Candida* species, namely *C. parapsilosis, C. tropicalis, C. guilliermondii* and *C. krusei* were used to evaluate the comprehensive anticandidal ability, and they showed similar drug susceptibility like *C. albicans* and *C. glabrata* (Table 3). Their activities against different *Candida* strains especially to *C. krusei* was comparable to fluconazole. Six clinical isolates were also applied in this study. As shown in Table 3, compounds **c1**-**c4** all showed fluconazole-comparable activity to fluconazole sensitive strains but inert towards fluconazole resistant isolates. There are multi-aspect reasons for azoles resistance. Overexpression or point mutation of *ERG11* gene and increase of efflux pumps like Cdr1p and Mdr1p are the most frequently cause find in *Candida* spp. [9,20]. The overexpression of efflux pump was relatively more possible to be response for the inert of **c1**-**c4**, since the efflux pumps with broad substrates could significantly decrease their intracellular concentration. The two fluconazole-resistant strains (S381 and CA422 in Table 3) were thereafter quantified for their expression of *CDR1* and *CDR2* genes which were more than 10 times overexpressed when comparing to the reference one (data not shown), thus explaining the inactive of **c1**-**c4**.

2.2.2. The cytotoxicity assessment

Fungi is eukaryote like mammalian cells, which means side effects might be caused by antifungal agents. It is thus necessary to consider the toxicity of **c1**-**c5** and **g1**-**g3**. Human normal liver cell line LO2 was used for the *in vitro* cytotoxicity evaluation. All the eight compounds did not display considerable toxicity at 100 μg/mL which demonstrated

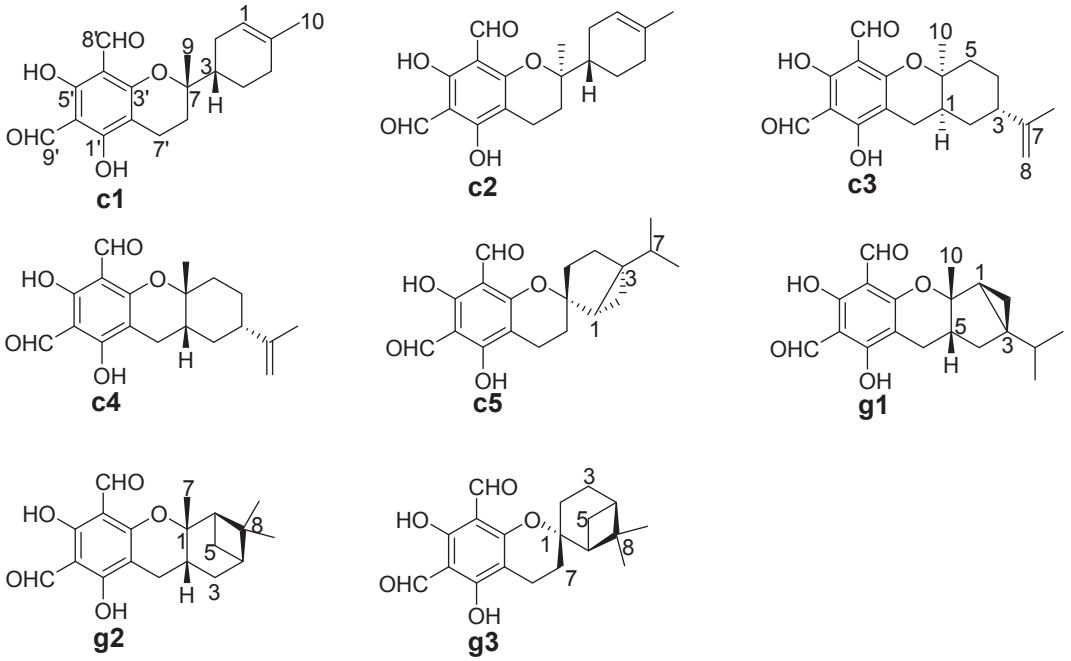

Fig. 2. Structures of compounds **c1-c5** and **g1-g3.**

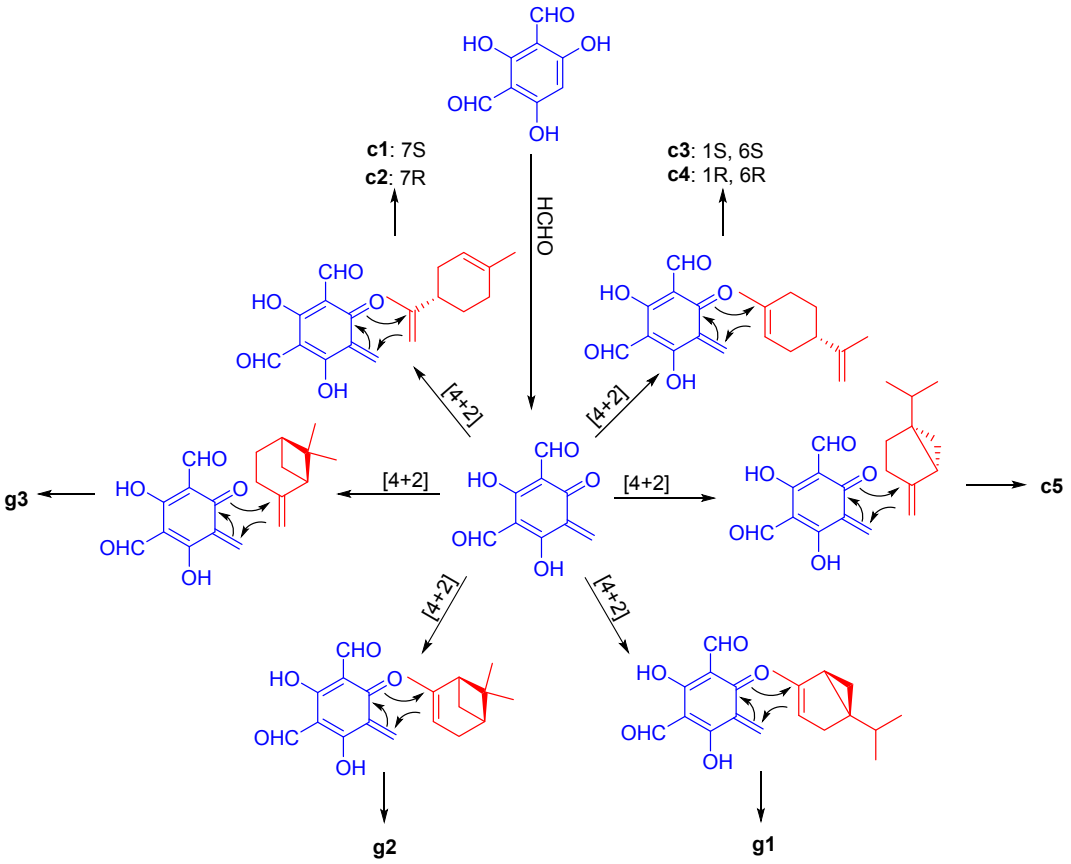

Scheme 2. The formation of compounds **c1**-**c5** and **g1**-**g3**.

Table 2
In vitro anticandidal activity of the compounds **c1-c5** and **g1-g3**.

Compounds	*C. albicans*[a]	*C. glabrata*[a]
c1	16.97 ± 1.16	10.17 ± 1.09
c2	8.65 ± 1.33	13.51 ± 2.20
c3	> 50	20.27 ± 1.09
c4	17.17 ± 2.60	22.78 ± 4.52
c5	> 50	21.40 ± 3.17
g1	21.64 ± 4.07	> 50
g2	23.19 ± 3.45	> 50
g3	> 50	28.74 ± 4.92
Fluconazole[b]	0.50 ± 0.24	1.00 ± 0.10

C. albicans (SC5314); *C. glabrata* (ATCC 15126).
[a] MIC_{50} value; μg/mL.
[b] Positive drug.

these compounds are safety at their active concentration ranges (Fig. S4).

2.2.3. The in vitro C. albicans biofilms inhibition of c2

Biofilms are a protected niche for microorganisms, where they are inherently tolerant to antimicrobial treatment. The current antifungal agents are low in susceptibility of *Candida* biofilms [37–38]. Given the severity of biofilm-related diseases, antibiofilm activity is an important capability for potential antifungal candidates. A series of bioassays were therefore carried out to evaluate the biofilm inhibition of **c2**. The crystal violet (CV) method was used to see if **c2** could prevent biofilm formation. As shown in Fig. 3, about 50% and 66% suppression were obtained at the concentrations of 12.5 and 25 μg/mL respectively. The biofilm growth was obviously disrupted upon **c2** treatment and the antibiofilm effect started from the biofilm initiation stage. In another assay using mature biofilm, **c2** was also found to effectively eliminate the mature biofilms that had grown for 24 h in a dose dependent way. When treated with 100 μg/mL **c2**, almost all mature biofilms (90%) were removed. Above experimental results revealed that compound **c2** could prevent *C. albicans* biofilm formation and disrupt mature biofilm effectivity.

2.2.4. Observating the c2 treated biofilms under microscopy

To provide visualized evidence, the antibiofilm effect was further confirmed by the analysis of confocal laser scanning microscopy (CLSM) and scanning electron microscopy (SEM). As shown in Figs. 4a and 5a to c, the long filaments developed into an expanding network in the control group. After the treatment of **c2**, a disruption was found and enhanced in a dose-dependent manner. In the CLSM results visualized by fluorescein diacetate, the dead hyphae labeled in red was significantly increased at the concentration of 25 μg/mL, and a large proportion of dead hyphae was found in the treating group of 50 μg/mL **c2**. These results clearly demonstrated that the viability of hypha reduced as **c2** increased (Fig. 4c and d). In the SEM analysis, we found that the biofilm of control group (Fig. 5a–c) developed long and tightly twisted filaments and the cells density were large. In the **c2** treatment group, cells were found being restricted at the budding yeast stage and the density of biofilm cells was consequently reduced (Fig. 5k and l). When increasing **c2**, the hypha decreased and yeast increased. When the **c2** concentration increased to 50 μg/mL, few long hyphae were seen, which indicated that **c2** could block hyphal elongation and filamentation. These results demonstrated that **c2** can reduce cell viability and it inhibited biofilm by locking *C. albicans* in the yeast form of the growth.

Table 3
In vitro anticandidal activity of the compounds **c1-c4**.

Strains	c1	c2	c3	c4	Fluconazole[b]
C. parapsilosis[a]	6.12 ± 1.21	4.80 ± 3.24	7.07 ± 1.83	12.41 ± 3.91	1.60 ± 0.92
C.tropicalis[a]	11.90 ± 2.41	5.20 ± 1.47	19.07 ± 4.32	12.30 ± 3.71	0.90 ± 0.01
C. guilliermondii[a]	4.56 ± 0.32	9.89 ± 2.74	9.93 ± 2.74	4.78 ± 1.02	2.50 ± 0.81
C.krusei[a]	7.16 ± 1.73	5.32 ± 1.72	7.55 ± 1.92	7.59 ± 2.95	8.00 ± 2.78
YEM12[a]	4.72 ± 3.87	2.94 ± 0.15	12.93 ± 2.75	10.12 ± 3.72	0.50 ± 1.89
YEM14[a]	> 50	22.05 ± 0.23	> 50	> 50	30.00 ± 0.03
CA21[a]	10.02 ± 4.21	5.74 ± 1.31	4.45 ± 1.67	12.41 ± 4.72	1.00 ± 0.06
CA13[a]	10.68 ± 3.21	9.13 ± 2.52	8.88 ± 2.86	12.30 ± 4.21	1.00 ± 0.11
S381[a]	> 50	> 50	> 50	> 50	> 50
CA422[a]	> 50	> 50	> 50	> 50	> 50

C. parapsilosis (ATCC 22019); *C. tropicalis* (ATCC 750); *C. guilliermondii* (ATCC 6260); *C. krusei* (ATCC 1182).
YEM12, YEM14, CA21, CA13, S381 and CA422 are clinical isolates of *C. albicans.*
[a] MIC_{50} value; μg/mL.
[b] Positive drug.

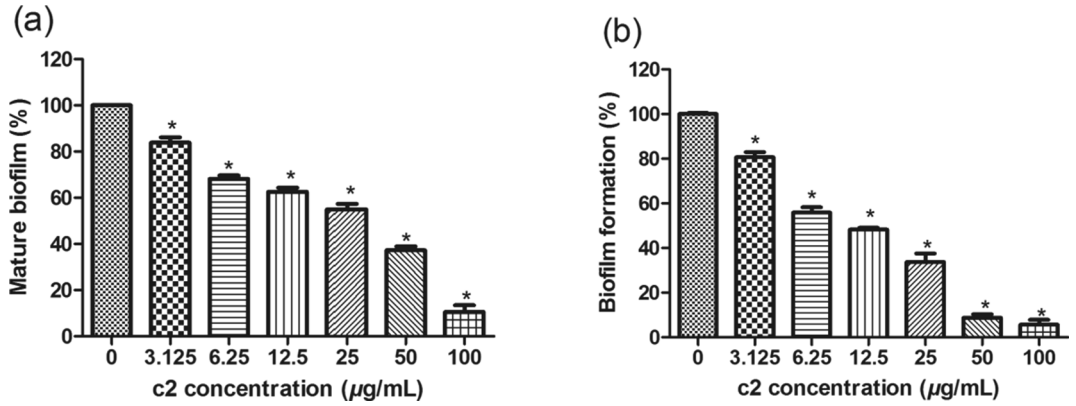

Fig. 3. C2 inhibits *C. albicans* biofilms *in vitro*. (a) Effects of different concentrations of **c2** on mature biofilm. (b) Effects of different concentrations of **c2** on biofilm formation. Bars represent means ± SDs from three experiments. *, P < 0.05.

3. Conclusion

Enlightened by the diversity-oriented synthesis, commercially available essential oils that are abundant in terpenes were applied as reagents in the biomimetic synthesis of FPMs, which generated various FPMs in one reaction. The following antifungal bioassay-guided isolation successfully led to eight anticandidal FPMs. Compound **c2**, one limonene-derived FPM, is the most active one. It has a broad-spectrum anticandidal ability which was powerfully comparable to fluconazole when testing against several *Candida* strains *in vitro*. Compound **c2** also possesses the antibiofilm activity which was evidenced by blocking hyphal elongation and filamentation. These qualities make **c2** a promising candidate for further antifungal-based structure modification.

4. Experimental section

4.1. Chemistry

Reagents and solvents were purchased from common commercial suppliers and were used without further purification. Progress of the reaction was monitored by TLC using silica gel plates with fluorescence GF254 (Qingdao Haiyang Chemical Plant, Qingdao, China) and the compounds on the TLC plates were detected under UV light. Column chromatography was performed on silica gel (200–300 mesh). Optical rotations were measured with a JASCO P-1020 spectropolarimeter. The ECD spectra was recorded using a JASCO 810 spectropolarimeter. The HRESIMS spectra was measured using an Agilent UPLC-Q-TOF analyser. Analytical HPLC was performed using an Agilent 1260 Series instrument with a DAD detector and shim-pack VP-ODS (250 × 4.6 mm). Preparative HPLC was performed using a Shimadzu LC-6AD Series instrument with a shim-pack RP-C_{18} (20 × 200 mm). Nuclear magnetic resonance (^{1}H NMR and ^{13}C NMR) spectra were recorded on a Bruker AVIII-500 and Bruker AVIII-600 spectrometer with TMS as an internal standard.

4.1.1. General procedure for the synthesis of 2,4-diformyl phloroglucinol

2,4-diformyl phloroglucinol was synthesized as described in the literature [24].

Phosphoryl chloride (8 mL, 83.5 mmol) was added dropwise to DMF (6.5 mL, 83.5 mmol) with strong stirring, at room temperature under a nitrogen atmosphere. The mixture was stirred for 30 min. This Vilsmeier reagent was then slowly added to a stirred solution of anhydrous phloroglucinol (5 g, 39.5 mmol) in dioxane (25 mL) at ambient temperature, under a nitrogen atmosphere. This reaction mixture was stirred further for 12 h, and it turned into a yellow solid. This solid mixture was cooled to 0 °C before being added to ice-water slurry (~200 mL), and stirring was continued for a further 4 h, during which time a salmon colored precipitate formed. This crude product was then filtered off and purified by silica gel column chromatography using petroleum ether/ethyl acetate (3:1) as eluent to get 2,4-diformyl phloroglucinol (5.9 g); cream colored solid; yield 82%. ^{1}H NMR (DMSO-d_6, 500 MHz) δ ppm 5.91 (s, 1H, Ar-H), 10.02 (s, 2H, CHO), 12.51 (br s., 2H, OH), 13.53 (br s., 1H, OH).

4.1.2. General procedure for the synthesis of compounds (c1-c6, g1-g7)

A mixture of 2,4-diformyl phloroglucinol (1 g, 5.5 mmol), formaldehyde (1.1 mL, 11 mmol), essential oil (3.75 mL, 16.5 mmol) and sodium acetate (4.5 g, 55 mmol) in acetic acid (30 mL) was stirred under 100 °C for 16 h. Then, the reaction mixture was cooled to room temperature. The saturated sodium bicarbonate solution (20 mL) was

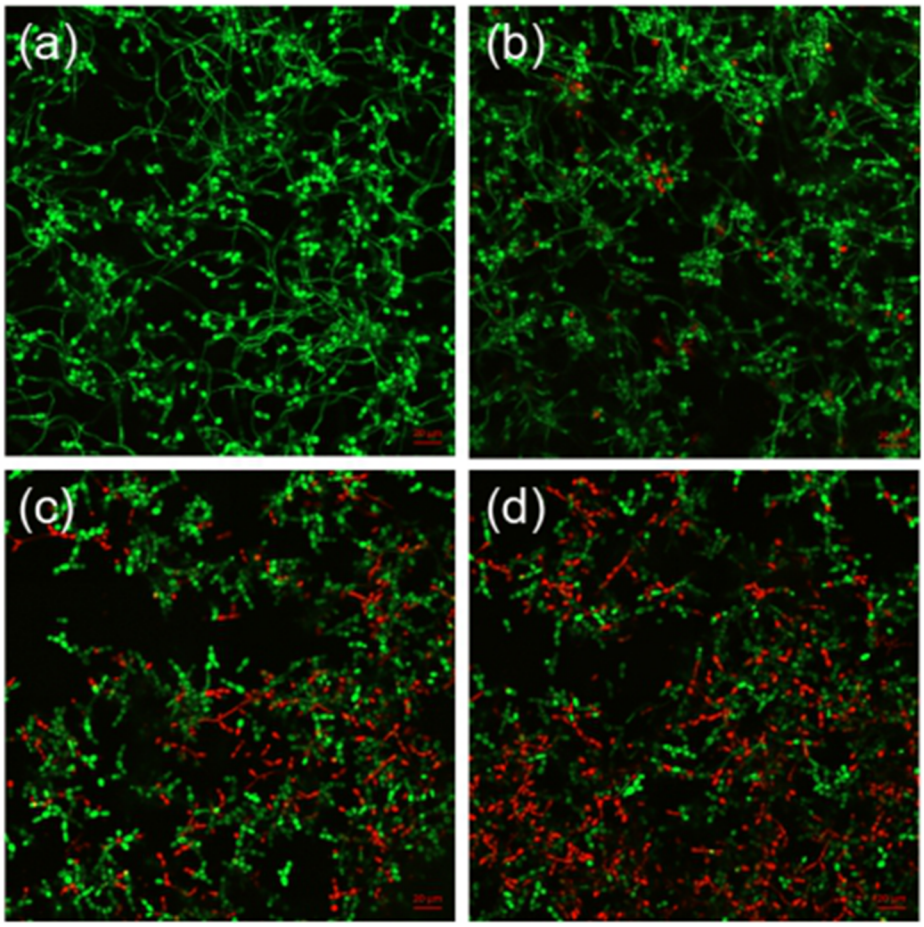

Fig. 4. Confocal laser scanning microscopy images of *C. albicans* biofilms developed *in vitro*. The healthy cells with an intact membrane were stained with fluorescent green and the cells with damaged membranes stained fluorescent red. (a) Control group; (b) 12.5 μg/mL **c2**; (c) 25 μg/mL **c2**; (d) 50 μg/mL **c2**. (For interpretation of the references to colour in this figure legend, the reader is referred to the web version of this article.)

added to neutralize excess acid. The mixture was extracted with CH_2Cl_2 (3 × 10 mL), and the combined organic layers were washed with brine (20 mL) and dried over Na_2SO_4. Filtration and removal of the solvent under reduced pressure afforded a yellow oil. Then, the 12 crude products were separated by silica gel chromatography with petroleum ether/ethyl acetate (100:1 to 1:1, *v/v*) and divided into 4 fractions which were then submitted to anticandidal activity assay. The best anticandidal activity fractions (fraction A from cedar oil's product and fraction B from ginger oil's product) were subject to chromatographic separation by a reversed-phase C_{18} column to obtain fractions A1-A2 (MeOH/H_2O, 60:40/100:0, *v/v*) and fractions B1-B3 (MeOH/H_2O, 55:45/100:0, *v/v*). Fraction A1 was purified using preparative HPLC with 87% acetonitrile in water to obtain compounds **c1** (23 mg), **c2** (34 mg), **c6** (46 mg). Fraction A2 was separated by HPLC using the mobile phase MeCN/H_2O (90:10, *v/v*) to give compounds **c3** (33 mg), **c4** (38 mg), **c5** (13 mg). Fraction B1 was subjected to preparative HPLC (MeCN/H_2O, 85:15, *v/v*) to obtain compounds **g1** (14 mg), **g2** (37 mg), **g3** (19 mg). Fraction B2 was purified by preparative HPLC with 78% acetonitrile in water to obtain compounds **g4** (42 mg) and **g6** (39 mg). Fraction B3 was further separated by HPLC (MeCN/H_2O, 70:30, *v/v*) affording compounds **g5** (26 mg) and **g7** (31 mg).

Cedartriol A (**c1**): White power. 23 mg. $[\alpha]_D^{25}$ + 15.5 (*c* 0.11, MeOH). ^{1}H NMR (500 MHz, $CDCl_3$) δ ppm 13.44 (s, 1H, 1′-OH) 13.25 (s, 1H, 5′-OH) ,10.16 (s, 1H, H-9′), 10.05 (s, 1H, H-8′), 5.38 (dd, J = 4.1, 1.0 Hz, 1H, H-1), 2.60 (dt, J = 16.8, 6.3 Hz, 1H, H-7′), 2.52 (m, 1H, H-7′), 2.07 (m, 1H, H-5), 2.00 (m, 1H, H-2), 1.98 (m, 1H, H-8), 1.93 (m, 1H, H-4), 1.89 (m, 1H, H-5), 1.86 (m, 1H, H-3), 1.85 (m, 1H, H-8), 1.80 (m, 1H, H-4), 1.65 (s, 3H, H-10), 1.30 (s, 3H, H-9), 1.26 (m, 1H, H-2). ^{13}C NMR (125 MHz, $CDCl_3$) δ ppm 192.1 (C-8′), 191.8 (C-9′), 169.0 (C-3′), 168.3 (C-1′), 163.3 (C-5′), 134.7 (C-6), 119.7 (C-1), 104.4 (C-6′), 103.8 (C-4′), 100.6 (C-2′), 82.7 (C-7), 41.6 (C-3), 30.7 (C-2), 27.4 (C-4), 26.6 (C-5), 23.5 (C-8), 23.4 (C-10), 20.2 (C-9), 14.7 (C-7′). HRESIMS *m/z* 329.1397 $[M-H]^-$ (calcd for $C_{19}H_{22}O_5$, 329.1394).

Cedartriol B (**c2**): White power. 34 mg. $[\alpha]_D^{25}$ + 18.2 (*c* 0.09, MeOH). ^{1}H NMR (500 MHz, $CDCl_3$) δ ppm 13.44 (s, 1H, 1′-OH), 13.25 (s, 1H, 5′-OH), 10.15 (s, 1H, H-9′), 10.03 (s, 1H, H-8′), 5.04 (br d, J = 3.7, 1H, H-1), 2.63 (dt, J = 16.7, 6.0 Hz, 1H, H-7′), 2.51 (m, 1H, H-7), 2.08 (m, 1H, H-5), 2.03 (m, 1H, H-2), 2.01 (m, 1H, H-8), 1.94 (m, 1H, H-4), 1.94 (m, 1H, H-5), 1.85 (m, 1H, H-3), 1.85 (m, 1H, H-8), 1.81 (m, 1H, H-4), 1.66 (s, 3H, H-10), 1.36 (m, 1H, H-2), 1.29 (s, 3H, H-9). ^{13}C NMR (125 MHz, $CDCl_3$) δ ppm 192.4 (C-8′), 192.0 (C-9′), 168.8 (C-1′), 168.5 (C-3′), 163.5 (C-5′), 134.0 (C-6), 120.1 (C-1), 104.4 (C-6′), 103.5 (C-4′), 100.1 (C-2′), 81.0 (C-7), 42.0 (C-3), 30.6 (C-2), 27.8 (C-4), 26.7 (C-5), 23.9 (C-8), 23.9 (C-10), 22.0 (C-9), 15.0 (C-7′). HRESIMS *m/z* 329.1392 $[M-H]^-$ (calcd for $C_{19}H_{22}O_5$, 329.1394).

Cedartriol C (**c3**): White power. 33 mg. $[\alpha]_D^{25}$ + 34.8 (*c* 0.09, MeOH). ^{1}H NMR (500 MHz, $CDCl_3$) δ ppm 13.46 (s, 1H, 1′-OH), 13.27 (s, 1H, 5′-OH), 10.15 (s, 1H, H-9′), 10.06 (s, 1H, H-8′), 4.86 (br s, 1H, H-8), 4.80 (br s, 1H, H-8), 2.65 (dd, J = 16.9, 6.3 Hz, 1H, H-7), 2.47 (dd, J = 16.9, 7.0 Hz, 1H, H-7), 2.34 (br s, 1H, H-3), 2.02 (m, 1H, H-1), 1.85 (m, 1H, H-2), 1.85 (m, 1H, H-4), 1.81 (m, 1H, H-5), 1.78 (m, 1H, H-4), 1.75 (s, 3H, H-9), 1.67 (m, 1H, H-2), 1.67 (m, 1H, H-5), 1.43 (s, 3H, H-10). ^{13}C NMR (125 MHz, $CDCl_3$) δ ppm 192.2 (C-8′), 191.7 (C-9′), 169.2 (C-3′), 168.3 (C-1′), 162.9 (C-5′), 147.3 (C-7), 110.4 (C-8), 104.1 (C-6′), 103.9 (C-4′), 99.5 (C-2′), 80.8 (C-6), 38.0 (C-3), 33.1 (C-4), 32.8 (C-1), 31.8 (C-2), 26.3 (C-5), 25.7 (C-10), 21.9 (C-9), 20.6 (C-7′). HRESIMS *m/z* 329.1396 $[M-H]^-$ (calcd for $C_{19}H_{22}O_5$, 329.1394).

Cedartriol D (**c4**): White power. 38 mg. $[\alpha]_D^{25}$ + 30.3 (*c* 0.09, MeOH). ^{1}H NMR (500 MHz, $CDCl_3$) δ ppm 13.45 (s, 1H, 1′-OH), 13.26 (s, 1H, 5′-OH), 10.15 (s, 1H, H-9′), 10.07 (s, 1H, H-8′), 4.67 (br s, 1H, H-8), 4.64 (br s, 1H, H-8), 2.73 (dd, J = 16.9, 6.5 Hz, 1H, H-7′), 2.42 (br d, J = 16.9, 1H, H-7′), 2.15 (m, 1H, H-5), 2.02 (m, 1H, H-3), 1.91 (m,

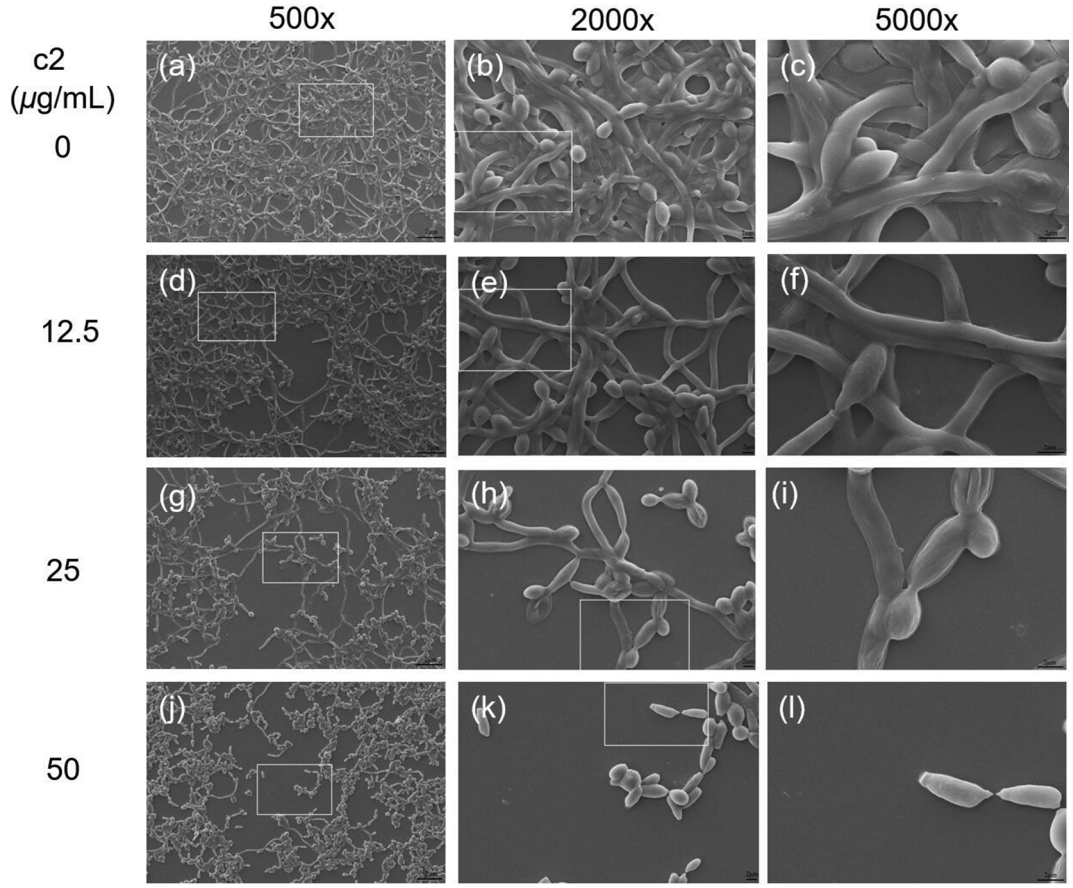

Fig. 5. Scanning electron microscopy images of *C. albicans* biofilms treated with different concentrations of **c2**. The inset in the 500×, 2000× panels show the area that was magnified.

1H, H-1), 1.68 (s, 3H, H-9), 1.65 (m, 2H, H-4), 1.61 (m, 1H, H-5), 1.52 (m, 1H, H-2), 1.30 (s, 3H, H-10), 1.12 (m, 1H, H-2). ^{13}C NMR (125 MHz, $CDCl_3$) δ ppm 192.1 (C-8′), 191.8 (C-9′), 169.6 (C-3′), 168.3 (C-1′), 162.8 (C-5′), 149.3 (C-7), 109.0 (C-8), 104.3 (C-6′), 104.1 (C-4′), 98.9 (C-2′), 78.7 (C-6), 44.4 (C-3), 38.3 (C-5), 35.6 (C-1), 33.5 (C-2), 26.8 (C-4), 25.4 (C-10), 22.1 (C-7′), 21.0 (C-9). HRESIMS *m/z* 329.1398 $[M-H]^-$ (calcd for $C_{19}H_{22}O_5$, 329.1394).

Cedartriol E (**c5**): White power. 13 mg. $[\alpha]_D^{25}$ + 14.5 (*c* 0.10, MeOH). ^{1}H NMR (500 MHz, $CDCl_3$) δ ppm 13.44 (s, 1H, 1′-OH), 13.25 (s, 1H, 5′-OH), 10.16 (s, 1H, H-9′), 10.03 (s, 1H, H-8′), 2.67 (dt, *J* = 16.6, 6.5 Hz, 1H, H-7′), 2.53 (dt, *J* = 16.6, 6.3 Hz, 1H, H-7′), 1.98 (m, 1H, H-4), 1.91 (m, 1H, H-10), 1.87 (m, 1H, H-10), 1.81 (m, 1H, H-5), 1.67 (m, 1H, H-4), 1.38 (m, 1H, H-7), 1.33 (m, 1H, H-5), 1.33 (m, 1H, H-1), 0.97 (d, *J* = 7.0, 1H, H-9), 0.96 (d, *J* = 7.0, 1H, H-8), 0.54 (m, 1H, H-2), 0.39 (m, 1H, H-2). ^{13}C NMR (125 MHz, $CDCl_3$) δ ppm 192.2 (C-8′), 191.8 (C-9′), 169.1 (C-3′), 168.4 (C-2′), 163.6 (C-5′), 104.5 (C-6′), 103.9 (C-4′), 101.1 (C-2′), 91.2 (C-6), 34.9 (C-3), 33.3 (C-5), 32.5 (C-7), 30.3 (C-1), 27.6 (C-10), 25.3 (C-4), 20.2 (C-9), 19.8 (C-8), 16.5 (C-7′), 13.4 (C-2). HRESIMS *m/z* 329.1398 $[M-H]^-$ (calcd for $C_{19}H_{22}O_5$, 329.1394).

Gingertriol A (**g1**): White power. 14 mg. $[\alpha]_D^{25}$ + 29.2 (*c* 0.08, MeOH). ^{1}H NMR (500 MHz, $CDCl_3$) δ ppm 13.47 (s, 1H, 1′-OH), 13.25 (s, 1H, 5′-OH), 10.14 (s, 1H, H-9′), 10.09 (s, 1H, H-8′), 2.63 (br d, *J* = 16.9, 1H, H-7′), 2.41 (dd, *J* = 16.6, 6.5 Hz, 1H, H-7′), 1.92 (m, 1H, H-5), 1.71 (dd, *J* = 12.6, 7.5 Hz, 1H, H-4), 1.45 (m, 1H, H-1), 1.43 (m, 1H, H-4), 1.39 (s, 3H, H-10), 1.33 (m, 1H, H-7), 0.87 (d, *J* = 6.9, 3H, H-8), 0.83 (d, *J* = 6.9, 3H, H-9), 0.58 (m, 1H, H-2), 0.57 (m, 1H, H-2). ^{13}C NMR (125 MHz, $CDCl_3$) δ ppm 192.1 (C-8′), 191.6 (C-9′), 169.5 (C-3′), 168.3 (C-1′), 162.6 (C-5′), 103.9 (C-6′), 103.8 (C-4′), 98.1 (C-2′), 89.3 (C-6), 34.6 (C-5), 33.5 (C-3), 32.6 (C-1), 32.4 (C-7), 31.1 (C-4), 22.1 (C-10), 20.1 (C-9), 19.7 (C-8), 16.2 (C-7′), 14.3 (C-2). HRESIMS *m/z* 329.1398 $[M-H]^-$ (calcd for $C_{19}H_{22}O_5$, 329.1394).

Gingertriol B (**g2**): White power. 37 mg. $[\alpha]_D^{25}$ + 16.2 (*c* 0.10, MeOH). ^{1}H NMR (500 MHz, $CDCl_3$) δ ppm 13.36 (s, 1H, 1′-OH), 13.20 (s, 1H, 5′-OH), 10.16 (s, 1H, H-9′), 9.95 (s, 1H, H-8′), 2.71 (m, 1H, H-2), 2.69 (m, 1H, H-7′), 2.45 (dd, *J* = 15.5, 6.1 Hz, 1H, H-7′), 2.26 (t, *J* = 5.6, 1H, H-6), 2.15 (br s, 1H, H-3), 2.13 (m, 1H, H-5), 1.90 (br dd, *J* = 9.4, 4.0 Hz, 1H, H-4), 1.48 (s, 3H, H-7), 1.33 (m, 1H, H-3), 1.31 (s, 3H, H-10), 1.10 (s, 3H, H-9), 0.79 (d, *J* = 10.6, 1H, H-5). ^{13}C NMR (125 MHz, $CDCl_3$) δ ppm 192.1 (C-8′), 191.8 (C-9′), 168.9 (C-3′), 168.4 (C-1′), 166.3 (C-5′), 104.0 (C-6′), 103.9 (C-4′), 100.6 (C-2′), 88.5 (C-1), 54.9 (C-6), 40.7 (C-4), 40.5 (C-8), 34.2 (C-3), 31.9 (C-2), 28.9 (C-7), 28.3 (C-10), 28.0 (C-5), 22.9 (C-9), 19.7 (C-7′). HRESIMS *m/z* 329.1397 $[M-H]^-$ (calcd for $C_{19}H_{22}O_5$, 329.1394).

Gingertriol C (**g3**): White power. 19 mg. $[\alpha]_D^{25}$ + 21.9 (*c* 0.08, MeOH). ^{1}H NMR (500 MHz, $CDCl_3$) δ ppm 13.43 (s, 1H, 1′-OH), 13.23 (s, 1H, 5′-OH), 10.15 (s, 1H, H-9′), 10.03 (s, 1H, H-8′), 2.56 (t, *J* = 6.7, 1H, H-7′), 2.26 (m, 1H, H-2), 2.16 (m, 1H, H-4), 2.03 (m, 1H, H-7), 2.01 (m, 1H, H-6), 1.98 (m, 1H, H-5), 1.97 (m, 1H, H-3), 1.92 (m, 1H, H-3), 1.86 (m, 1H, H-7), 1.60 (m, 1H, H-2), 1.30 (s, 3H, H-10), 1.26 (m, 1H, H-5), 1.02 (s, 3H, H-9), 0.88 (m, 1H, H-7′). ^{13}C NMR (125 MHz, $CDCl_3$) δ ppm 192.2 (C-8′), 191.8 (C-9′), 168.9 (C-3′), 168.3 (C-1′), 163.8 (C-5′), 104.6 (C-6′), 103.7 (C-4′), 100.8 (C-2′), 85.7 (C-1), 49.8 (C-4), 40.7 (C-6), 39.4 (C-8), 31.8 (C-7), 28.7 (C-5), 27.6 (C-10), 26.7 (C-2), 24.8 (C-3), 23.4 (C-9), 14.9 (C-7′). HRESIMS *m/z* 329.1393 $[M-H]^-$ (calcd for $C_{19}H_{22}O_5$, 329.1394).

4.2. Agar disk diffusion test

Disk diffusion test was performed as previously described [19]. In brief, 500 μL *C. albicans* (SC5314) suspension (5×10^5 cells/mL) was spread uniformly onto yeast peptone dextrose (YPD) agar plates. A plate with 1% DMSO was used as the vehicle control. The 6-mm-diameter

filter disks contain different content crude product (200 μg, 100 μg, 50 μg) was placed onto the agar surface. The plates were incubated for 24 h at 35 °C and then measure the growth inhibition zones. Images were collected by using Chemidoc XRS +.

4.3. In vitro antifungal assay

The minimum inhibitory concentrations (MIC) of compounds against fungal were determined by the broth microdilution method based on the Clinical and Laboratory Standards Institute (CLSI) standard M27-A3 [39]. A range of concentrations from 50 to 1.5625 μg/mL for synthesised compounds were made in RPMI 1640. One hundred microliter compound and 100 μL cells suspension with a final concentration of 2.5×10^3 cells/mL were added into 96-well plates. Fluconazole was used as positive control drugs. Then, the plates were incubated at 35 °C for 24 h. Optical densities at 540 nm (OD540) were measured by a microplate reader (Tecan SUNRISE) and the MIC_{50} was defined as the concentration of drugs that inhibited 50% of cell growth. All tests were repeated for three times. Compounds were dissolved in DMSO. The maximum amounts of DMSO that was added into the culture medium did not affect cell multiplication.

4.4. Cytotoxicity assay

Cytotoxicity was measured using the MTT [3-(4, 5- dimethylthiazol-2-yl)-2, 5-diphenyl tetrazolium bromide] method [40]. In brief, the LO2 (normal human hepatic cell line) cell lines were seeded into 96-well plates (10^4 cells/well). After incubating over night, the cells were treated with compounds and further incubated for 48 h at 37 °C. Then, the MTT solution was added to each well. After 4 h, DMSO was added to dissolve formazan crystals. The absorbance of wells was measured at 570 nm.

4.5. In vitro antibiofilm assay

The antibiofilm effect of **c2** was measured by a crystal violet (CV) assay [41]. In brief, 100 μL of *C. albicans* YEM12 cell suspension (1.0×10^6 cells/mL in RPMI 1640 medium) was placed into 96-well plates and incubated at 37 °C for 1.5 h for initial adhesion. The medium was aspirated and nonadherent cells were removed by washing with 100 μL of PBS. 100 μL RPMI 1640 medium with or without different concentrations of **c2** was added to each well and further incubated for 24 h. For detection of **c2** on mature biofilms, biofilms pregrown for 24 h were treated with different concentrations of **c2** and were incubated for 24 h at 37 °C. Then the content of each well was removed, wells were washed twice with PBS and fixed the cell with 99% methanol (200 μL) for 15 min. The 99% methanol was discarded, and each well was stained with 200 μL of 0.1% crystal violet solution followed by 30 min incubation at room temperature. Later, the excess crystal violet solution from the plates was removed, thoroughly washed with distilled water for 3 to 4 times and air dried at room temperature. The crystal violet stained biofilm was solubilized in 33% acetic acid (200 μL). Afterwards, 100 μL of the destaining solution was transferred to a new 96-well plate, and the absorbance was recorded at 570 nm. The experiments were carried out in triplicates.

4.6. Confocal laser scanning microscopy (CLSM) observations

CLSM was performed by using six-well plates containing plastic disks as previously reported [42–43]. Biofilms (*C. albicans* YEM12) were incubated in plates following the method described above. After incubation each well was washed with PBS, stained with 10 μg/mL fluorescein diacetate (FDA) and 5 μg/mL propidium iodide (PI) for 30 min and viewed under confocal laser scanning microscope (LSM800; Carl Zeiss).

4.7. Scanning electron microscopy (SEM) observations

SEM was performed to investigate the ultrastructure of *C. albicans* YEM12 biofilms [44–45]. Sterile glass disks coated with poly-L-lysine hydrobromide (Sigma) were used to incubate the biofilms. Then the medium of each well was removed, biofilms were washed with PBS and fixed with 2.5% glutaraldehyde for 2 h. Later, biofilms were rinsed twice in cacodylate buffer, garnished with 1% osmic acid for 2 h, dehydrated in an ascending ethanol series, treated with hexamethyldisilazane (Polysciences Europe GmbH, Eppelheim, Germany), and dried overnight. The specimens were coated with gold. Afterwards, the ultrastructure of the biofilms was visualized with a Carl Zeiss SEM (EVO LS10) in high-vacuum mode.

Declaration of Competing Interest

The authors declare that they have no known competing financial interests or personal relationships that could have appeared to influence the work reported in this paper.

Acknowledgements

This research work was funded by the National Natural Science Foundation of China (81773901), the Drug Innovation Major Project (2018ZX09711-001-007 and 2018ZX09735002-003) and the 111 Project from Ministry of Education of China and the State Administration of Foreign Export Affairs of China (B18056).

Appendix A. Supplementary material

Supplementary data to this article can be found online at https://doi.org/10.1016/j.bioorg.2020.104248.

References

[1] D.J. Newman, G.M. Cragg, J. Nat. Prod. 79 (2016) 629–661.
[2] L.L. Silver, Future Microbiol. 10 (2015) 1711–1718.
[3] D.W. Denning, Lancet. 362 (2003) 1142–1151.
[4] V. Moudgal, J. Sobel, Expert Opin. Pharmacother. 11 (2010) 2037.
[5] F. Benz, A. Knusel, J. Nuesch, H. Trelchler, W. Voser, Helvetica Chim. Acta 57 (1974) 2459–2477.
[6] T. Iwamoto, A. Fujie, K. Sakamoto, Y. Tsurumi, N. Shigematsu, M. Yamashita, S. Hashimoto, M. Okuhara, M. Kohsaka, J. Antibiot. 47 (1994) 1084–1091.
[7] E.M. Carmona, A.H. Limper, Clin. Chest Med. 38 (2017) 393–402.
[8] D. Allen, D. Wilson, R. Drew, J. Perfect, Expert Rev. Anti-infect. Ther. 13 (2015) 787–798.
[9] N.M. Revie, K.R. Iyer, N. Robbins, L.E. Cowen, Curr. Opin. Microbiol. 45 (2018) 70–76.
[10] D. Marchaim, L. Lemanek, S. Bheemreddy, K.S. Kaye, J.D. Sobel, Obstet. Gynecol. 120 (2012) 1407–1414.
[11] N. Liu, J. Tu, G.Q. Dong, Y. Wang, C.Q. Sheng, J. Med. Chem. 61 (2018) 5484–5511.
[12] S. Yin, J.J. Xue, C.Q. Fan, Z.H. Miao, J. Ding, J.M. Yue, Org. Lett. 9 (2007) 5549–5552.
[13] Y. Yu, L.S. Gan, S.P. Yang, L. Sheng, Q.F. Liu, S.N. Chen, J. Li, J.M. Yue, J. Nat. Prod. 79 (2016) 1365–1372.
[14] I.P. Singh, J. Sidana, S.B. Bharate, W.J. Fole, Nat. Product Reports 27 (2010) 393–416.
[15] Z.C. Shang, M.H. Yang, K.L. Jian, X.B. Wang, L.Y. Kong, Chem. Eur. J. 22 (2016) 11778–11784.
[16] Z.C. Shang, M.H. Yang, R.H. Liu, X.B. Wang, L.Y. Kong, Sci. Rep. 6 (2016) 39815.
[17] Z.C. Shang, C. Han, J.L. Xu, R.H. Liu, Y. Yin, X.B. Wang, M.H. Yang, L.Y. Kong, Phytochemistry. 163 (2019) 111–117.
[18] R.H. Liu, Z.C. Shang, T.X. Li, M.H. Yang, L.Y. Kong, Antimicrob. Agents Chemother. 61 (2017) 2707–2716.
[19] J.L. Xu, R.H. Liu, F.J. Sun, L. An, Z.C. Shang, L.Y. Kong, M.H. Yang, Front. Cell. Infect. Microbiol. 9 (2019) 211.
[20] W.Q. Chang, J. Liu, M. Zhang, H.Z. Shi, S. Zheng, S.Y. Jin, Y.H. Gao, S. Wang, A. Ji, H.X. Lou, Nat. Commun. 9 (2018) 5102.
[21] B.X. Liang, W.Y. Shao, C.G. Zhu, G.S. Wen, X. Yue, R.M. Wang, J.M. Quan, J. Du, X.Z. Bu, ACS Chem. Biol. 11 (2016) 425–434.
[22] L. Leanza, M. Romio, K.A. Becker, M. Azzolini, L. Trentin, A. Manago, E. Venturini, A. Zaccagnino, A. Mattarei, L. Carraretto, A. Urbani, S. Kadow, L. Biasutto, V. Martini, F. Severin, R. Peruzzo, V. Trimarco, J.H. Egberts, C. Hauser, A. Visentin, G. Semenzato, H. Kalthoff, M. Zoratti, E. Gulbins, C. Paradisi, I. Szabo, Cancer Cell.

31 (2017) 516–531.
[23] M. Fridman, R.I. Benhamou, M. Bibi, J. Berman, Angew. Chem. Int. Ed. 57 (2018) 6230–6235.
[24] A.L. Lawrence, R.M. Adlington, J.E. Baldwin, V. Lee, J.A. Kershaw, A.L. Thompson, Org. Lett. 12 (2010) 1676–1679.
[25] S.L. Schreiber, Science. 287 (2000) 1964–1969.
[26] M.D. Burke, S.L. Schreiber, Angew. Chem. Int. Ed. 43 (2004) 46–58.
[27] W.R.J. Galloway, I.L. Albert, R.S. David, Nat. Commun. 1 (2010) 80.
[28] Y.L. Zhang, C. Chen, X.B. Wang, L. Wu, M.H. Yang, J. Luo, C. Zhang, H.B. Sun, J.G. Luo, L.Y. Kong, Org. Lett. 18 (2016) 4068.
[29] L. Wu, J. Luo, X.B. Wang, R.J. Li, Y.L. Zhang, L.Y. Kong, RSC. Adv. 5 (2015) 93900–93906.
[30] L. Wu, J. Luo, Y.L. Zhang, M.D. Zhu, X.B. Wang, J.G. Luo, M.H. Yang, B.Y. Yu, H.Q. Yao, Y. Dai, Q.L. Guo, Y.J. Chen, H.B. Sun, L.Y. Kong, Tetrahedron Lett. 56 (2015) 229–232.
[31] J. Novak, C. Bitsch, J. Langbehn, F. Pank, M. Skoula, Y. Gotsiou, C. Frantz, Biochem. Synst. Ecol. 28 (2000) 697–704.
[32] M. Kozuka, T. Sawada, E. Mizuta, F. Kasahara, T. Amano, T. Komiya, M. Goto, Chem. Pharm. Bull. 30 (1982) 1964–1973.
[33] R.S. Xu, J.K. Snyder, K. Nakanishi, J. Am. Chem. Soc. 106 (1984) 734.
[34] Q. Cheng, J.K. Snyder, J. Org. Chem. 53 (1988) 4562–4567.
[35] R. Cai, M.M. Hu, Y.J. Zhang, C. Niu, T.L. Yue, Y.H. Yuan, Z.L. Wang, LWT-Food Sci. Technol. 106 (2019) 50–56.
[36] A. Thakre, G. Zore, S. Kodgire, R. Kazi, S. Mulange, R. Patil, A. Shelar, B. Santhakumari, M. Kulkarni, K. Kharat, S.M. Karuppayil, Med Mycol. 56 (2018) 565–578.
[37] M. Gulati, C.J. Nobile, Microbes Infect. 18 (2016) 310–321.
[38] Y. Lu, C. Su, H.P. Liu, Trends Microbiol. 22 (2014) 707–714.
[39] Clinical and Laboratory Standards Institute, Reference method for broth dilution antifungal susceptibility testing of yeasts, approved standard 3rd ed., Document M27-A3, Clinical and Laboratory Standards Institute, Wayne, PA, 2008.
[40] T. Mosmann, J. Immunol. Methods 65 (1983) 55–63.
[41] A. Bruder-Nascimento, C.H. Camargo, A.L. Mondelli, M.F. Sugizaki, T. Sadatsune, E. Bagagli, Braz. J. Microbiol. 45 (2014) 1371–1377.
[42] D.N. Jackson, L. Yang, S.B. Wu, E.J. Kennelly, P.N. Lipke, Antimicrob. Agents. Chemother. 59 (2015) 6032–6038.
[43] N.N. Mishra, S. Ali, P.K. Shukla, Braz. J. Infect. Dis. 18 (2014) 287–293.
[44] K.L. Lee, H.R. Buckley, C.C. Campbell, Sabouraudia. 13 (1975) 148–153.
[45] L.X. Zhao, D.D. Li, D.D. Hu, G.H. Hu, L. Yan, Y. Wang, Y.Y. Jiang, PLoS. One. 8 (2013) 79671.